Anal. Chem. **2010,** *82,* 282–289

Extractive Electrospray Ionization Mass Spectrometry for Sensitive Detection of Uranyl Species in Natural Water Samples

Mingbiao Luo,[†] Bin Hu,[†] Xie Zhang,[†] Daofeng Peng,[†] Huanwen Chen,*[,†] Lili Zhang,[‡] and Yanfu Huan*[,‡]

Department of Applied Chemistry, East China Institute of Technology, Fuzhou, Jiangxi Province 344000, P. R. China, and College of Chemistry, Jilin University, Changchun, Jilin Province 130021, P. R. China

Ambient mass spectrometry has been increasingly applied for sensitive detection of trace organic compounds present in complex matrixes. In the real world, detection of trace amounts of inorganic species, particularly with speciation information, is of great significances. Herein a method based on extractive electrospray ionization (EESI) tandem mass spectrometry (MS/MS) has been established for rapid detection of radioactive inorganic species in natural water samples. Negatively charged uranyl acetate undergoes characteristic fragmentation in the gas phase, providing the fundamental chemistry for specific detection of uranyl species in complex matrixes without sample pretreatment. Under the optimized experimental conditions, uranyl species in various natural water samples were rapidly detected using multiple-stage EESI mass spectrometry. The mean time for each sample analysis was about 10 s. The limit of detection was about a few 10^{-3} ng/L of uranium by utilizing the characteristic fragments obtained in the EESI-MS^3 experiments. The typical relative standard deviation (RSD) of this method was 6.9∼8.1% for 8 measurements (S/N = 3). The dynamic response range was 10^{-1}∼10^3 ng/L for uranium in water samples. The isotope ratio of uranyl species was quantitatively detected using EESI-MS experiments. The results show that EESI-MS, a typical method initially developed for organic compound analysis, has promising perspectives for real time, online monitoring of inorganic species such as uranyl species in natural water samples.

Driven by the practical needs of academic research and industrial production, an accelerating trend in modern analytical science is to perform trace analysis where the analyte concentration is of the order of parts per million or less. Serving as a powerful analytical platform for sensitive detection of analytes at trace levels, mass spectrometry, combined with other techniques if necessary, has been used as an irreplaceable tool for decades, due to the unparalleled sensitivity, premier specificity, and general applicability. Ambient mass spectrometry,[1−9] serving as a solution to the bottleneck of high-throughput mass spectrometric analysis, has dramatically improved the speed of mass spectrometric analysis of complex samples and thus successfully spread the mass spectrometric application across multiple disciplines. Typically, organic species involved in drug discovery,[10−12] organic chemistry,[13−16] material science,[17−19] and biology,[20−24] etc. have been characterized at molecular levels using ambient mass spectrometry. Because of the complexity of the matrixes of practical samples,

* Corresponding author. Dr. Huanwen Chen, Applied Chemistry Department, East China Institute of Technology, Fuzhou, Jiangxi Province 344000, P. R. China. Phone: (86)-794-8258-703. Fax: (86)-794-8258-320. E-mail: chw8868@gmail.com.

[†] East China Institute of Technology.

[‡] Jilin University.

(1) Takats, Z.; Wiseman, J. M.; Gologan, B.; Cooks, R. G. *Science* **2004**, *306*, 471–473.
(2) Chingin, K.; Chen, H. W.; Gamez, G.; Zhu, L.; Zenobi, R. *Anal. Chem.* **2009**, *81*, 123–129.
(3) Ifa, D. R.; Manicke, N. E.; Dill, A. L.; Cooks, R. G. *Science* **2008**, *321*, 805–805.
(4) Harper, J. D.; Charipar, N. A.; Mulligan, C. C.; Zhang, X.; Cooks, R. G.; Ouyang, Z. *Anal. Chem.* **2008**, *80*, 9097–9104.
(5) Andrade, F. J.; Shelley, J. T.; Wetzel, W. C.; Webb, M. R.; Gamez, G.; Ray, S. J.; Hieftje, G. M. *Anal. Chem.* **2008**, *80*, 2646–2653.
(6) Andrade, F. J.; Shelley, J. T.; Wetzel, W. C.; Webb, M. R.; Gamez, G.; Ray, S. J.; Hieftje, G. M. *Anal. Chem.* **2008**, *80*, 2654–2663.
(7) Cheng, C. Y.; Yuan, C. H.; Cheng, S. C.; Huang, M. Z.; Chang, H. C.; Cheng, T. L.; Yeh, C. S.; Shiea, J. *Anal. Chem.* **2008**, *80*, 7699–7705.
(8) Cody, R. B. *Anal. Chem.* **2009**, *81*, 1101–1107.
(9) Cooks, R. G.; Ouyang, Z.; Takats, Z.; Wiseman, J. M. *Science* **2006**, *311*, 1566–1570.
(10) Petucci, C.; Diffendal, J.; Kaufman, D.; Mekonnen, B.; Terefenko, G.; Musselman, B. *Anal. Chem.* **2007**, *79*, 5064–5070.
(11) Ma, X. X.; Zhao, M. X.; Lin, Z. Q.; Zhang, S. C.; Yang, C. D.; Zhang, X. R. *Anal. Chem.* **2008**, *80*, 6131–6136.
(12) Chen, H. W.; Talaty, N. N.; Takats, Z.; Cooks, R. G. *Anal. Chem.* **2005**, *77*, 6915–6927.
(13) Zhu, L.; Gamez, G.; Chen, H. W.; Huang, H. X.; Chingin, K.; Zenobi, R. *Rapid Commun. Mass Spectrom.* **2008**, *22*, 2993–2998.
(14) Chen, H.; Eberlin, L. S.; Nefliu, M.; Augusti, R.; Cooks, R. G. *Angew. Chem., Int. Ed.* **2008**, *47*, 3422–3425.
(15) Marquez, C. A.; Wang, H. Y.; Fabbretti, F.; Metzger, J. O. *J. Am. Chem. Soc.* **2008**, *130*, 17208–17210.
(16) Benassi, M.; Wu, C. P.; Nefliu, M.; Ifa, D. R.; Volny, M.; Cooks, R. G. *Int. J. Mass Spectrom.* **2009**, *280*, 235–240.
(17) Huang, M. Z.; Hsu, H. J.; Wu, C. I.; Lin, S. Y.; Ma, Y. L.; Cheng, T. L.; Shiea, J. *Rapid Commun. Mass Spectrom.* **2007**, *21*, 1767–1775.
(18) Venter, A.; Ifa, D. R.; Cooks, R. G.; Poehlein, S. K.; Chin, A.; Ellison, D. *Propellants, Explos., Pyrotech.* **2006**, *31*, 472–476.
(19) Whitson, S. E.; Erdodi, G.; Kennedy, J. P.; Lattimer, R. P.; Wesdemiotis, C. *Anal. Chem.* **2008**, *80*, 7778–7785.
(20) Yang, S. P.; Chen, H. W.; Yang, Y. L.; Hu, B.; Zhang, X.; Zhou, Y. F.; Zang, L. L.; Gu, H. W. *Chin. J. Anal. Chem.* **2009**, *37*, 315–318.
(21) Nemes, P.; Vertes, A. *Anal. Chem.* **2007**, *79*, 8098–8106.
(22) Meetani, M. A.; Shin, Y. S.; Zhang, S. F.; Mayer, R.; Basile, F. *J. Mass Spectrom.* **2007**, *42*, 1186–1193.
(23) Nemes, P.; Barton, A. A.; Li, Y.; Vertes, A. *Anal. Chem.* **2008**, *80*, 4575–4582.
(24) Wiseman, J. M.; Ifa, D. R.; Venter, A.; Cooks, R. G. *Nat. Protoc.* **2008**, *3*, 517–524.

10.1021/ac9019494
Published on Web 11/25/2009

tandem mass spectrometry experiments and selective ion/molecule reactions as well are normally employed to enhance the confidence for specific detection of targeted analytes such as explosives.[25−29] To date, most efforts have been made to develop methods using ambient ionization techniques for rapid detection of organic species. Studies employing ambient mass spectrometry for rapid detection of inorganic compounds have rarely been reported in the literature.

Inorganic analytes are typically accompanied by salts of high content and thus are not compatible with most commercially available ionization techniques when the salts have not been preseparated. After a matrix cleanup, inorganic compounds are usually detected using inductively coupled plasma (ICP) mass spectrometry[30−34] rather than ambient ionization techniques. Because of the nature of ICP, analytes including both organic and inorganic species are usually broken down to elemental species for further mass spectrometric analysis or spectroscopic measurement. The destructive feature of ICP makes ICPMS difficult to obtain speciation information of the analytes such as complexes formed between metallic ions and organic ligand. Thus, sample pretreatments using chemical speciation methods combining chemical separation procedures such as solvent extraction, ion exchange, or coprecipitation is usually required by ICPMS for speciation analysis.[34−39] However, such methods requiring sample pretreatments suffer from the fact that oxidation states of the analytes may be altered during the chemical separation due to, for example, acidification of the sample, contacting the sample with strongly complexing agents, or chemical impurities. Also, the delicate sample pretreatment methods compromise the throughput of analysis. Therefore, it is an urgent practical need to establish novel methodologies for rapid detection of uranium in the environment and as fast screening tools for the presence of isotopically enriched uranium with high sensitivity and high specificity.

Research on uranium, a ubiquitous long-term radioactive element, is of sustained interest in physics,[40,41] chemistry,[42−45] energy technology,[46,47] and life science.[48−50] Solution chemistry of uranium is dominated by uranyl speciation, which involves in processes ranging from nuclear fuel processing[51] and waste handling to mobility and fate in the geologic subsurface.[52] Understanding uranyl speciation is fundamental to predicting radionuclide behavior in the environment and resulting in ultimately control of radionuclide in nuclear waste-storage facilities. Thus, uranyl species' studies are certainly of great importance. Techniques including mass spectrometry,[53−56] vibrational spectroscopy,[47] and quantum calculations[42,57] have been employed to study uranyl ions in the gas phase. Theoretically, these techniques can be used to obtain speciation information of uranium in the solution phase; in these cases, however, the result interpretation is sometimes problematic since the speciation information of uranium is not easily accessible in a straightforward way.

Among ambient ionization techniques[1−9] available, extractive electrospray ionization (EESI)[58] was introduced in 2006 for direct, online analysis of liquid samples in real time. In EESI, neutral analytes present in raw samples are dispersed in a spatial cross section formed between a sample plume and an electrospray beam; thereby the analytes undergo interactions and collisions with the primary ions produced by electrospraying pure solvent (e.g., acetic acid/methanol−water solution) and then ionized for further mass analysis. Ion suppression is reduced in EESI by distributing the matrixes over a relatively wide section in a three-dimensional space. Another unique feature of EESI is that the neutral samples are safely isolated from any high voltage or direct bombardment by charged particles, thus EESI makes ionization of the analyte possible without subjecting it to a harsh environment, which minimizes the speciation changes caused by the chemical events such as redox reactions occurring in the pretreatment and/or

(25) Chen, H. W.; Hu, B.; Hu, Y.; Huan, Y. F.; Zhou, Z. Q.; Qiao, X. F. *J. Am. Soc. Mass Spectrom.* **2009**, *20*, 719–722.
(26) Justes, D. R.; Talaty, N.; Cotte-Rodriguez, I.; Cooks, R. G. *Chem. Commun.* **2007**, 2142–2144.
(27) Cotte-Rodriguez, I.; Chen, H.; Cooks, R. G. *Chem. Commun.* **2006**, 953–955.
(28) Takats, Z.; Cotte-Rodriguez, I.; Talaty, N.; Chen, H. W.; Cooks, R. G. *Chem. Commun.* **2005**, 1950–1952.
(29) Cotte-Rodriguez, I.; Hernandez-Soto, H.; Chen, H.; Cooks, R. G. *Anal. Chem.* **2008**, *80*, 1512–1519.
(30) Grinberg, P.; Willie, S.; Sturgeon, R. E. *Anal. Chem.* **2005**, *77*, 2432–2436.
(31) Grinberg, P.; Willie, S.; Sturgeon, R. E. *J. Anal. At. Spectrom.* **2005**, *20*, 717–723.
(32) Pozebon, D.; Dressler, V. L.; Becker, J. S.; Matusch, A.; Zoriy, M.; Becker, J. S. *J. Anal. At. Spectrom.* **2008**, *23*, 1281–1284.
(33) Rodrigues, J. L.; Nunes, J. A.; Batista, B. L.; De Souza, S. S.; Barbosa, F. *J. Anal. At. Spectrom.* **2008**, *23*, 992–996.
(34) McSheehy, S.; Sperling, M. *Spectroscopy* **2009**, *24*, 14–18.
(35) Kuczewski, B.; Marquardt, C. M.; Seibert, A.; Geckeis, H.; Kratz, J. V.; Trautmann, N. *Anal. Chem.* **2003**, *75*, 6769–6774.
(36) May, C. C.; Worsfold, P. J.; Keith-Roach, M. J. *TrAC, Trends Anal. Chem.* **2008**, *27*, 160–168.
(37) Chassaigne, H.; Vacchina, V.; Lobinski, R. *TrAC, Trends Anal. Chem.* **2000**, *19*, 300–313.
(38) Zhang, N.; Suleiman, J. S.; He, M.; Hu, B. *Talanta* **2008**, *75*, 536–543.
(39) Yang, G. D.; Xu, J. H.; Zheng, J. P.; Xu, X. Q.; Wang, W.; Xu, L. J.; Chen, G. N.; Fu, F. F. *Talanta* **2009**, *78*, 471–476.
(40) Sobiczewski, A.; Pomorski, K. *Prog. Part. Nucl. Phys.* **2007**, *58* (1), 292–349.
(41) Gibson, J. K. *Int. J. Mass Spectrom.* **2002**, *214*, 1–21.
(42) Buhl, M.; Diss, R.; Wipff, G. *J. Am. Chem. Soc.* **2005**, *127*, 13506–13507.
(43) Groenewold, G. S.; Cossel, K. C.; Gresham, G. L.; Gianotto, A. K.; Appelhans, A. D.; Olson, J. E.; Van Stipdonk, M. J.; Chien, W. *J. Am. Chem. Soc.* **2006**, *128*, 3075–3084.
(44) Hagberg, D.; Karlstrom, G.; Roos, B. O.; Gagliardi, L. *J. Am. Chem. Soc.* **2005**, *127*, 14250–14256.
(45) Schadel, M. *Angew. Chem., Int. Ed.* **2006**, *45*, 368–401.
(46) Gibson, J. K.; Marcalo, J. *Coord. Chem. Rev.* **2006**, *250*, 776–783.
(47) Groenewold, G. S.; Gianotto, A. K.; Cossel, K. C.; Van Stipdonk, M. J.; Moore, D. T.; Polfer, N.; Oomens, J.; de Jong, W. A.; Visscher, L. *J. Am. Chem. Soc.* **2006**, *128*, 4802–4813.
(48) Ansoborlo, E.; Prat, O.; Moisy, P.; Den Auwer, C.; Guilbaud, P.; Carriere, M.; Gouget, B.; Duffield, J.; Doizi, D.; Vercouter, T.; Moulin, C.; Moulin, V. *Biochimie* **2006**, *88*, 1605–1618.
(49) Van Horn, J. D.; Huang, H. *Coord. Chem. Rev.* **2006**, *250*, 765–775.
(50) Karpas, Z.; Lorber, A.; Elish, E.; Kol, R.; Roiz, Y.; Marko, R.; Katorza, E.; Halicz, L.; Riondato, J.; Vanhaecke, F.; Moens, L. *Health Phys.* **1998**, *74*, 337–345.
(51) Greenwood, N. N.; Earnshaw, A. *Chemistry of the Elements*, 2nd ed.; Butterworth Heinemann: Oxford, Great Britain, 1997.
(52) Brooking, D. G. *Geochemical Aspects of Radioactive Waste Disposal*; Springer-Verlag: New York, 1984.
(53) Pasilis, S.; Somogyi, A.; Herrmann, K.; Pemberton, J. E. *J. Am. Soc. Mass Spectrom.* **2006**, *17*, 230–240.
(54) Anbalagan, V.; Chien, W.; Gresham, G. L.; Groenewold, G. S.; Van Stipdonk, M. J. *Rapid Commun. Mass Spectrom.* **2004**, *18*, 3028–3034.
(55) Van Stipdonk, M. J.; Chien, W.; Anbalagan, V.; Gresham, G. L.; Groenewold, G. S. *Int. J. Mass Spectrom.* **2004**, *237*, 175–183.
(56) Chien, W.; Anbalagan, V.; Zandler, M.; Van Stipdonk, M.; Hanna, D.; Gresham, G.; Groenewold, G. *J. Am. Soc. Mass Spectrom.* **2004**, *15*, 777–783.
(57) Zhang, Z. Y.; Pitzer, R. M. *J. Phys. Chem. A* **1999**, *103*, 6880–6886.
(58) Chen, H. W.; Venter, A.; Cooks, R. G. *Chem. Commun.* **2006**, 2042–2044.

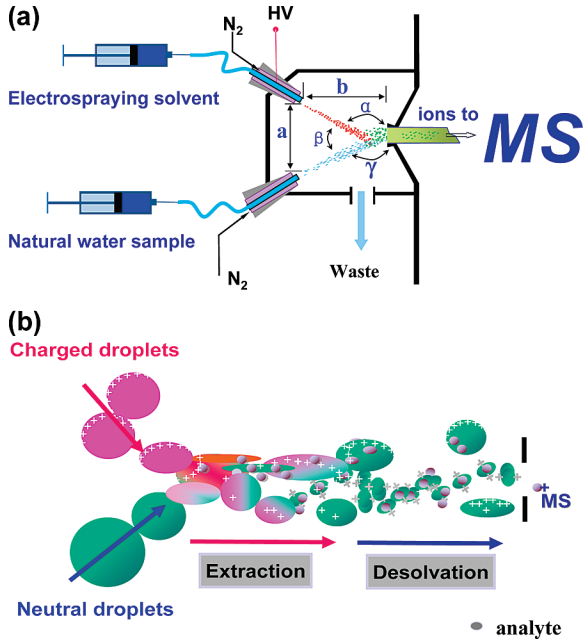

Figure 1. EESI-MS spectrometry for sensitive detection of radioactive species: (a) schematic diagram of the EESI source and (b) schematic illustration of ion formation in the EESI process. Charged droplets generated by the electrospray impact the neutral sample droplets to initialize the microdroplet−droplet extraction process, during which charge exchange occurs to generated charged analytes. The solvated analyte ions then undergo the desolvation process to produce analyte ions.

ionization steps.[14,16,59] Among many types of analyzers available, ion traps hold advantages such as high sensitivity, relatively low cost, and wide availability and provide the most competitive capability for performing multiple-stage mass spectrometry in a single device. Therefore, EESI has been implemented in an ion trap mass spectrometer for direct analysis of uranyl species in natural water samples without any sample pretreatment.

EXPERIMENTAL SECTION

Instrumental Setup. Under the negative ion detection mode, experiments were carried out using a LTQ-XL mass spectrometer (Finnigan, San Jose, CA) equipped with a homemade EESI source. The principle and basic configuration of an EESI source were previously illustrated for rapid analysis of liquid samples.[58,60] Briefly, the EESI source described here was developed for detection of radioactive species, with improved safety. As schematically shown in Figure 1a, the EESI assembly was air-tight enclosed to the LTQ mass spectrometer, so that no material can be released into the ambient air when the radioactive sample was infused into the EESI source. In the EESI source, the neutral analytes underwent numerous collisions with the charged particles generated by the electrospray using a negative high voltage (−4 kV). During the collisions, online droplet−droplet extraction[15] occurred between the neutral sample droplets and the charged droplets (shown in Figure 1b), allowing continuous extraction of interesting compounds and subsequent ionization of neutral analytes. The analyte ions were then introduced into the LTQ mass analyzer for mass analysis through the ion guide system of the LTQ-MS instrument. The distance (a) between the end-tips of the two sprays and the distance (b) between the spray tips of the EESI source and the MS inlet was 2 and 5 mm, respectively. The angle (α) between the electrospray beam and the MS inlet of the LTQ-MS instrument and the angle (β) between the two spray beams was 150° and 60°, respectively. Thus, the angle (γ) was determined to be 150° as well. The LTQ-MS instrument was running in the negative ion detection mode. The temperature of the heated capillary of the LTQ-MS was maintained at 180 °C. The default values of voltages were used for the heating capillary, the tube lenses, the conversion dynodes, the detectors, etc. Further optimization was not performed.

All the full scan mass spectra were recorded using Xcalibur software of the LTQ-MS instrument with an average time of 30 s. The precursor ions of interest were isolated using a mass window of 1.4 mass/charge (m/z) unit. Collision-induce dissociation (CID) experiments were performed by applying 15−30% collision energy for 30 ms to the precursor ions. MS^n spectra were collected with a recording time more than 30 s if necessary. Compounds of interest were identified using MS and CID data matching of the unknown compounds against authentic standards.

Materials and Reagents. Uranyl acetate samples (A.R. grade) were gifts from the China Institute of Atomic Energy (Beijing, China). Chemicals such as methanol (A.R. grade) and acetic acid (A.R. grade) were bought from Chinese Chemical Reagent Co. Ltd. (Shanghai, China). All chemicals were directly used without any pretreatment, unless dissolution and dilution with deionized water when it was necessary. Deionized water with 1.0% acetic acid (v/v) containing no uranium was used as the blank water sample. Uranyl acetate was precisely added into blank water samples to make a series of dilute uranyl acetate standards. For actual sample analysis, the natural water samples were obtained from three different sites including a well, lake, and river, in which upstream is a uranium ore. To ensure the acetic acid ligand (Ac^-) was sufficient for the uranyl species in the natural water samples (5 mL, pH 6), 0.05 mL of pure acetic acid was added into each of the samples. After shaking for about 20 s, the resulting mixture was directly infused at a flow rate of 5 μL/min for EESI-MS analysis, without any further treatment. A methanol/water/acetic acid solution (40:40:20, v/v/v) was delivered at a flow rate of 5 μL/min to the ESI emitter, by using a syringe pump, for generation of the primary ions.

Safety Remarks. The handling of radioactive substances requires special permission. The complete EESI system had to be built as a ventilation hood coupled to the LTQ-MS instrument; and the waste, the exhaust of the LTQ-MS, was carefully collected for proper handling by another nuclear chemistry lab. One must be sure that no radionuclides are emitted into the laboratory atmosphere. Furthermore, the complete EESI system was equipped with an interlock switch in order to avoid contact with any high voltage by opening the ventilation hood.

RESULTS AND DISCUSSION

EESI-MS Spectrum of Uranyl Acetate. In the EESI mass spectrum recorded using a dilute uranyl acetate solution (≤0.01 μM), only one abundant peak is present at m/z 447 (Figure 2a),

(59) Sparrapan, R.; Eberlin, L. S.; Haddad, R.; Cooks, R. G.; Eberlin, M. N.; Augusti, R. *J. Mass Spectrom.* **2006**, *41*, 1242–1246.
(60) Gu, H. W.; Chen, H. W.; Pan, Z. Z.; Jackson, A. U.; Talaty, N.; Xi, B. W.; Kissinger, C.; Duda, C.; Mann, D.; Raftery, D.; Cooks, R. G. *Anal. Chem.* **2007**, *79*, 89–97.

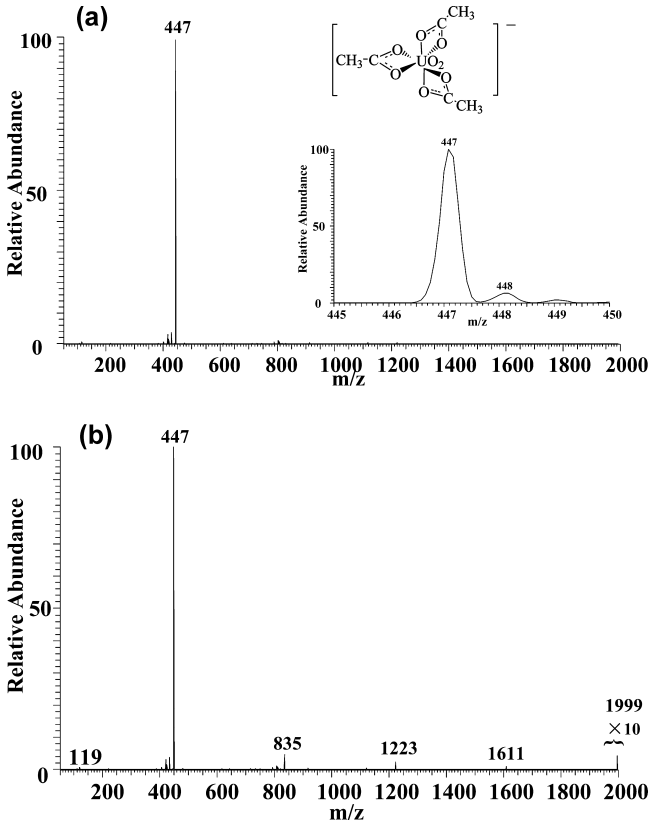

Figure 2. EESI-MS spectrum of uranyl acetate water solutions: (a) low concentration of uranyl acetate (0.01 μM). The inset shows the isotopic peak (6.3%) at *m/z* 488; (b) high concentration of uranyl acetate (1 μM).

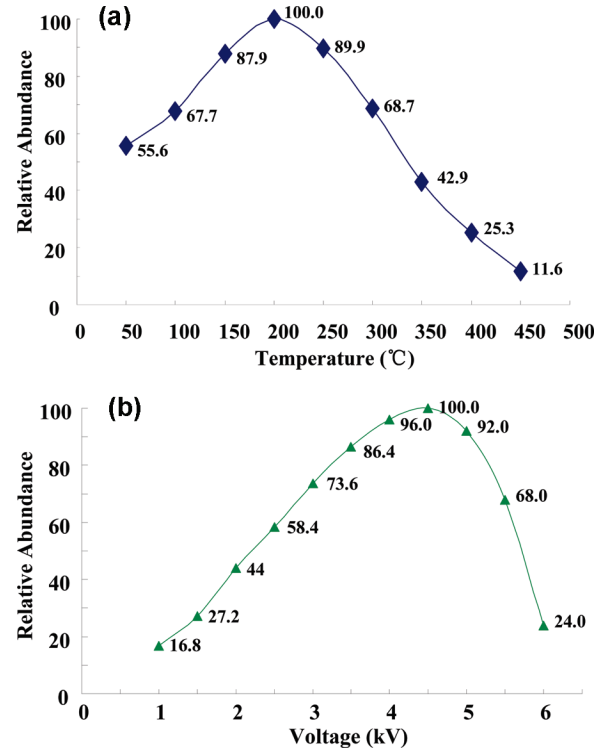

Figure 3. Optimization of the source temperature and the ESI voltage for uranyl acetate detection: (a) effect of the temperature of the heated capillary on the signal intensity of the peak at *m/z* 447; (b) effect of the high voltage on the signal intensity of the peak at *m/z* 447. Note that the signal intensities were normalized to 100% based on the highest signal detected. Each point designates an average of 10 measurements.

which correspond to the deprotonated uranyl acetate complex ($UO_2(Ac)_3^-$, Ac = CH_3COO). A small peak at *m/z* 119 (≤3%) was also shown in the EESI mass spectrum (Figure 2a) due to the formation of deprotonated acetic acid dimers in the EESI process. When a uranyl acetate aqueous solution with a relatively high concentration (≥1 μM) was directly infused to the EESI source, a series of ionic uranyl acetate clusters formulated as $(UO_2(Ac)_2)_nAc^-$ ($n = 1-5$) were detected at *m/z* 447, 835, 1223, 1611, and 1999 (Figure 2b), respectively. These peaks were not detected in the EESI mass spectrum recorded using low concentration solutions, probably because the initial concentration (e.g., 0.01 μM) was not high enough for the EESI process to form ionic clusters containing more than two uranyl species. When the methanol/water/acetic acid solution was electrosprayed, the spectral pattern (data not shown) did not vary along the concentrations of acetic acid in the sample solution because the acetic acid in the electrospray solution was enough for the complex formation.

Many reagents can be used in the ESI spray to generate the primary ions for EESI purpose. In this study, for the uranyl standard solutions, no considerable difference was detected when the composition of the electrospray solution varied from pure methanol to methanol/water/acetic acid. For natural water samples, a relatively low level signal was observed using solvent without acetic acid, probably in the natural water sample there were other ligands which competed with the Ac^- ligands from forming $(UO_2(Ac)_3)^-$ complex. Therefore, a mixture of methanol/water/acetic acid (40:40:20) was used for further experiments. It was also found that, in a relatively wide range, the variety of the acidity of the uranyl acetate solution (pH = 1−10) produced no considerable difference in the EESI mass spectrum.

The temperature of the heated capillary of the LTQ instrument affects the intensities of the $(UO_2(Ac)_2)_nAc^-$ ($n = 1-5$) clusters. Below 180 °C, the signal intensity (*m/z* 447) increased slightly along with the rise of the temperature (Figure 3a), probably due to the improved desolvation of the ions. The abundances of the $(UO_2(Ac)_2)_nAc^-$ ($n = 2-5$) clusters decreased notably when the temperature was beyond 200 °C, due to the thermal dissociation of the clusters.

The effect of the high voltage for the ESI on the signal levels of *m/z* 447 was plotted as shown in Figure 3b. Below −4 kV, the signal intensity (*m/z* 447) increased obviously when the ESI voltage was increased, probably because more primary ions were created when the ESI voltage was increased. The abundances of the signals dropped down significantly when the ESI voltage was higher than −5 kV, probably because the ions were accelerated by the electric field more than necessary, resulting in more astray ions which could not be guided into the mass analyzer.

Fragmentation of Uranyl Acetate in the Gas Phase. Upon CID in the gas phase (1×10^{-5} torr, 15% collision energy (CE)), the ions of *m/z* 447 lose neutral radicals ($CH_3COO^\bullet$), which results in a product of a radical anion of *m/z* 388 (Figure 4a). The cleavage of the radical ($CH_3COO^\bullet$) from the precursor ions indicates that the molecular residue (i.e., $UO_2(Ac)_2$) has a strong electron affinity. This is consistent with the observation that the radical anion (*m/z* 388) can be retained in the gas

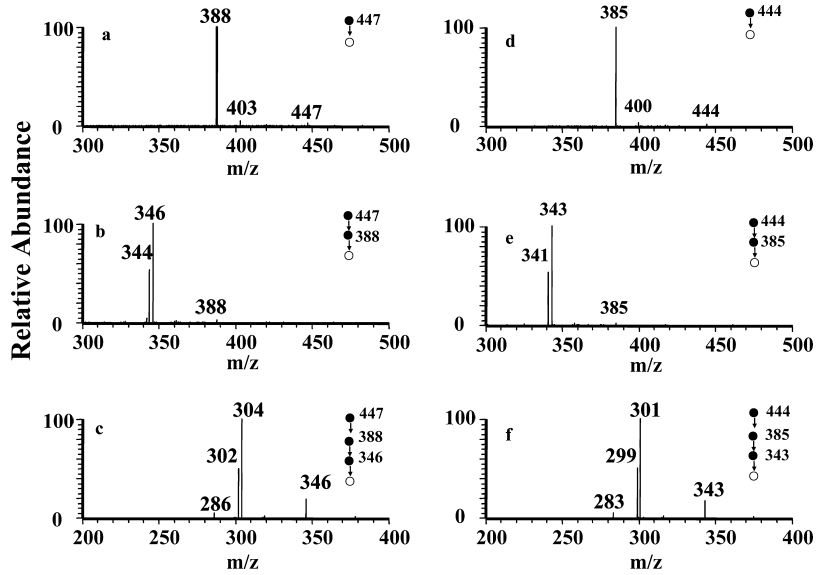

Figure 4. The intrinsic fragmentation pathways of uranyl acetate (*m*/*z* 447) was validated using ^{235}U isotope labeled compounds: (a) MS^2 spectrum of *m*/*z* 447; (b) MS^3 spectrum of *m*/*z* 388; (c) MS^4 spectrum of *m*/*z* 346; (d) MS^2 spectrum of *m*/*z* 444; (e) MS^3 spectrum of *m*/*z* 385; and (f) MS^4 spectrum of 343.

phase for a long time ($t \geq 10$ s). With relatively high collision energy (≥22%), the cleavage of CO_2 from the acetate group produced a small peak at *m*/*z* 403 in the CID mass spectrum of the precursor ions of *m*/*z* 447. The low relative abundance (~1%) of the peak at *m*/*z* 403 suggested this pathway was not favored under the experimental conditions. The radical anion (*m*/*z* 388) loses CH_2=C=O and CO_2, respectively, to produce the fragments at *m*/*z* 346 or *m*/*z* 344 (Figure 4b) in the MS^3 experiment. The major fragment of *m*/*z* 346 yields abundant product ions of *m*/*z* 304, 302, and 286 (Figure 4c) by the loss of CH_2=C=O and CO_2, respectively. Interestingly, only one fragment of *m*/*z* 286 (UO_3^-) was observed, due to the loss of water or methane, in further CID experiments using either *m*/*z* 304 or 302 as the precursor ions. The final product of the CID experiments (i.e., UO_3^-) gives no fragmentation in the CID experiment. Similar to the previous findings,[61] these data show that the UO_3^- species is intrinsically stable with respect to electron autodetachment and thermal fragmentation in the gas phase. The detail mechanism of the dissociation will be explicitly illustrated elsewhere using quantum chemistry tools combining systematic gas-phase CID and ion/molecule reactions studies. Scheme 1 summarizes the dissociation pathways observed using the uranyl acetate complex (*m*/*z* 447).

Validation of Fragmentation Paths. Identical fragmentation patterns were obtained using the ^{235}U isotope labeled uranyl acetate. As shown in Figure 4d–f, on each stage, the fragments observed were in good agreement with those obtained using ^{238}U uranyl species, showing that the dissociation pathways summarized in Scheme 1 are correct.

One remarkable feature of multiple-stage mass spectrometric analysis is the capability to explicit molecular structures of analytes. False positive signals can be eliminated by comparison with the multiple-stage mass spectral data using authentic compounds. Tandem mass spectrometry is required when a raw

Scheme 1. Fragmentation Pathways and Fragments of $[UO_2(CH_3COO)_3]^-$ in the Gas Phase[a]

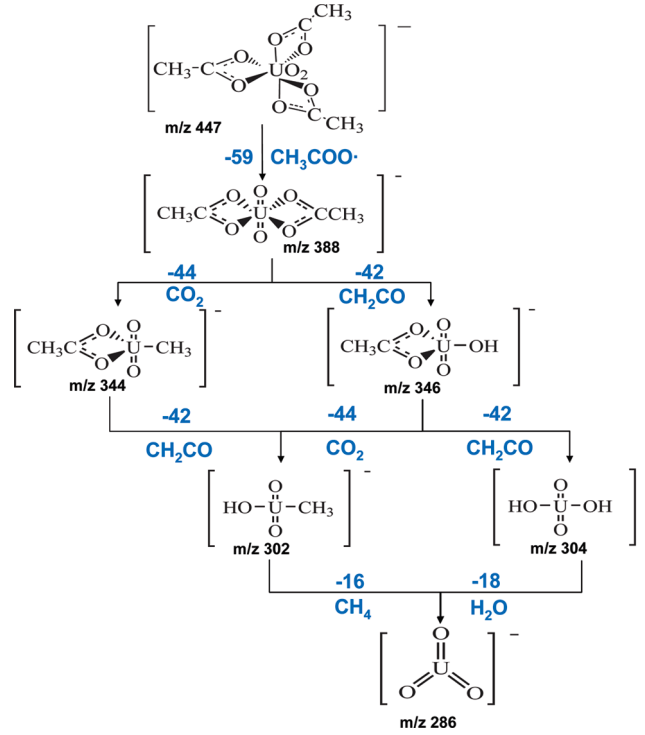

[a] Note that the structures shown here are only postulated structures for the negatively charged ions, which should be validated using other methods such as theoretical calculations.

sample is infused for ionization without cleaning up the complex matrixes.[20,62–65] In this work, the uranyl acetate clusters (*m*/*z*

(61) Marçalo, J.; Santos, M.; Pires de Matos, A.; Gibson, J. K. *Inorg. Chem.* **2009**, *48*, 5055–5057.

(62) Harris, G. A.; Nyadong, L.; Fernandez, F. M. *Analyst* **2008**, *133*, 1297–1301.

(63) Ifa, D. R.; Jackson, A. U.; Paglia, G.; Cooks, R. G. *Anal. Bioanal. Chem.* **2009**, *394*, 1995–2008.

(64) Manicke, N. E.; Wiseman, J. M.; Ifa, D. R.; Cooks, R. G. *J. Am. Soc. Mass Spectrom.* **2008**, *19*, 531–543.

(65) Yang, S. P.; Ding, J. H.; Zheng, J.; Hu, B.; Li, J. Q.; Chen, H. W.; Zhou, Z. Q.; Qiao, X. L. *Anal. Chem.* **2009**, *81*, 2426–2436.

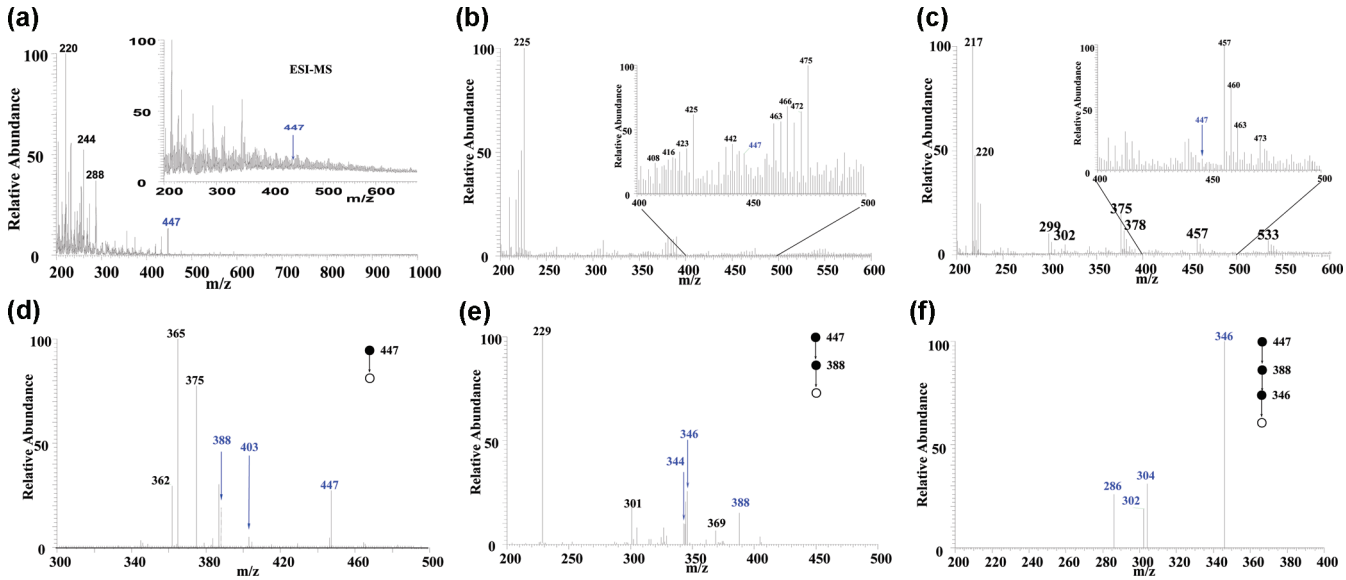

Figure 5. Direct analysis of natural water samples: (a) full scan mass spectrum of a river water sample. The inset shows the mass spectrum obtained using the same sample and direct infusion ESI-MS and (b) full scan mass spectrum of a lake water sample. The inset shows the zoomed-view of the peak at *m*/*z* 447 and (c) full scan mass spectrum of a well water sample. The inset shows the zoomed view of the peak at *m*/*z* 447; (d) MS^2 spectrum of *m*/*z* 447 detected in the river water sample; (e) MS^3 spectrum of *m*/*z* 388; (f) MS^4 spectrum of *m*/*z* 346 showing the fragmentation pattern identical to that shown in Figure 4c.

447) were dissociated when subjecting to collisions and produced the characteristic fragmentation patterns, which serve as a fundamental chemistry base for specific detection of uranyl species in mixtures with complex matrixes.

Direct Detection of Uranyl Species in Natural Water Samples. Following the procedure described in the Experimental Section, three water samples including river water, lake water, and well water were directly analyzed using EESI-MS. The full scan EESI mass spectra of the three samples were shown in Figure 5a–c, respectively. Among the numerous peaks that showed up in the mass spectra (Figure 5a), an abundant peak at *m*/*z* 447 (4.6×10^3 cps) was detected from the river water sample, with a good signal-to-noise ratio (S/N = 1500). However, no abundant signal was detected at *m*/*z* 447 when the same sample was directly infused to a commercial ESI source, although many peaks appeared in the ESI-MS spectrum (inset of Figure 5a). This was because the matrixes of the actual water sample were too complex for the ESI source. A much cleaner spectrum was obtained using EESI rather than ESI, because the ESI may produce more signals of matrix and background compounds since these two techniques are based on different mechanisms. For the rest of the two samples, the signal of uranyl (i.e., *m*/*z* 447) was not predominantly detected in the full scan mass spectra. However, the signal (*m*/*z* 447) was detectable ($\sim 9.6 \times 10^2$ cps), as shown in the zoomed view of the grassy mass spectra (the insets of Figure 5b,c). In such a case, multiple-stage CID experiments were performed to validate the signals. Figure 5d shows the MS/MS spectrum of the precursor ions of *m*/*z* 447, detected from the river water sample. It is no doubt that the characteristic fragments (i.e., *m*/*z* 388, 403) showed up in the spectrum but with relatively low intensities. In comparison with the MS/MS spectrum obtained using an authentic uranyl acetate sample, there are abundant peaks irrelevant to uranyl acetate. Thus it requires obtaining further characteristic fragmentation to improve the specificity. Figure 5e shows the major fragments of the precursor ions of *m*/*z* 388, and the signals detected at *m*/*z* 229, 301 rather than peaks at *m*/*z* 344, 346 suggest the precursor ions of *m*/*z* 388 were not 100% pure fragments derived from the uranyl acetate precursors. Figure 5f shows the CID spectrum of the signal at *m*/*z* 346, showing all characteristic fragments which are identical to the ones (Figure 4c) obtained using the authentic compound. The differential spectral pattern was caused by the different fragmentation conditions (less collision energy was used for collecting Figure 5f). Note that Figure 5f also suggests that the precursor ions (i.e., *m*/*z* 346) observed in the MS^3 spectrum were all associated with the uranyl species. For each stage of the fragmentation experiments, similar fragmentation patterns were correspondingly observed using the precursor ions of *m*/*z* 447 detected from different samples. With these distinctive fragments obtained, it is safe to use the signal at *m*/*z* 346 observed in the MS^3 spectrum for quantitative analysis. However, for ultimate specificity, it is recommended to validate the purity of the fragment observed at *m*/*z* 346 using further CID experiments, especially when the sample matrixes differ from our cases.

Detection Limit and Reproducibility. The characteristic signal of *m*/*z* 346 observed in the MS^3 spectrum was selected for quantitative measurement of uranyl species in water. Uranyl species are found widely in natural water at levels of about tens of parts per thousand. Using this method, we found uranyl signals from all the natural samples tested. Thus deionized water was used in our experiments to prepare the standard uranyl solutions for making the calibration curve. As shown in Figure 6a, a dynamic response was obtained between the signal of *m*/*z* 304 and the concentration of the uranyl acetate water solution using logarithmic scales. The linear equation was $y = 0.2664x + 3.8$ ($R^2 = 0.978$), providing a dynamic response range of 5 orders of magnitudes (10^{-1}~10^3 ng/L). The signal

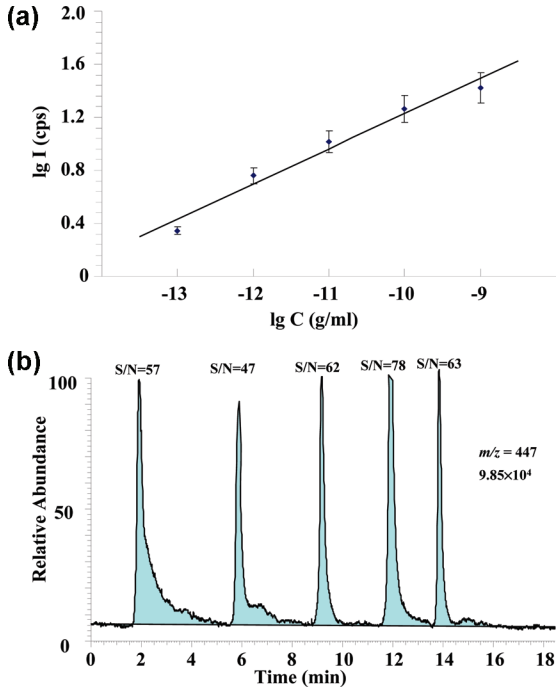

Figure 6. Signal responses of uranyl acetate obtained using EESI-MS^n. (a) The plots of the signal abundances of the fragment (m/z 346) obtained in MS^3 vs sample concentration, showing a dynamic response range between 0.10 and 1.0 × 10^3 ng/L. The bar symbols designate 5% of the mean values. The intercept of the calibration curve is not a zero, indicating that the limit of detection is much lower than the concentration of 0.10 ng/L. This is also in agreement with the LOD data; (b) single ion chromatogram of m/z 447 of 5 measurements.

Table 1. Analytical Results of Uranyl Species Analysis Using EESI-MS^n

sample	content measured[a] (ng/L)	values added (ng/L)	total content measured[a] (ng/L)	values found[a] (ng/L)	RSD[b] (%)	recovery (%)[c]
river water	450	100	530	80	8.1	80
well water	63	10	74	11	6.9	110
lake water	82	10	91	9	7.4	90

[a] Mean values of eight measurements. [b] RSD for eight measurements. [c] Recovery was calculated using the formula: recovery = [(total content measured − value added)/content added] × 100%.

response was not directly linear to the concentration of the analyte, probably because the signal was obtained using MS^3 experiments. The concentrations of the uranyl species in different natural water samples were quantitatively measured using this calibration curve. Table 1 summarizes the analytical results. As shown in Table 1, the recovery obtained using this method ranged 80%~110%, showing that this method is useful for quantitative detection of uranyl species in water. The limit of detection (LOD) of this method was found to be 2.33 × 10^{-3} ng/L, which is comparable to that reported with inductively coupled plasma mass spectrometry[66] and is much lower than the levels of uranium in natural waster.

Figure 6b shows the chromatograms of the selected ions (m/z 447) recorded using a uranyl acetate solution (1.0 × 10^3 ng/L).

(66) Becker, J. S. *Int. J. Mass Spectrom.* **2005**, *242*, 183–195.

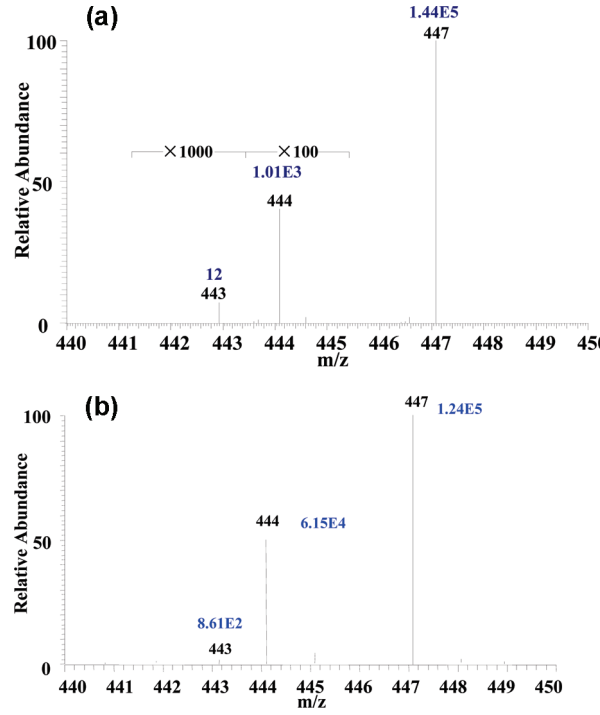

Figure 7. Rapid detection of isotope ratios of uranyl species by EESI-MS: (a) mass spectra with the natural ^{235}U/^{238}U isotope ratio and an (b) unusually high ^{235}U/^{238}U ratio.

Clearly, the acceptable reproducibility was achieved using this method. The relatively standard deviation (RSD) was about 8% for multiple measurements (n = 5). These data show that the uranyl species can be directly quantified from natural samples with acceptable precision and accuracy.

Measuring the Isotope Ratio of Uranyl Species. Uranium has three natural isotopes. The ^{235}U, the most radioactive uranium isotope of 0.725% natural abundance, is used widely in nuclear power plants and might be abused by terrorists as massive weapons. Therefore, it is important to rapidly detect this species at ultralow levels. As shown in Figure 4, the ^{235}U species provide the same fragmentation pattern and thus can be detected using this method with multiple-stage CID experiments. A ^{235}U/^{238}U ratio higher than 0.725% usually indicates that the ^{235}U species has been artificially enriched intentionally. Therefore, the ^{235}U/^{238}U ratio can be a useful marker to identify the spots used for uranium separation and enrichment. Figure 7 shows mass spectra showing a natural ^{235}U/^{238}U isotope ratio (a) and unusually high ^{235}U/^{238}U ratio (b). The uranyl species for the isotopes of ^{234}U, ^{235}U, and ^{238}U were detected simultaneously at m/z 443, 444, and 447 (Figure 7a), with the signal intensities of 12, 1040, and 144 000 cps, respectively. These isotope peaks were identified using multiple-stage CID experiments (MS^3), which produced the same characteristic fragments as those shown in Figure 4 at the corresponding stage. The isotope abundance ratio detected from the nonenriched uranium sample was 100:0.725:0.005 (^{238}U/^{235}U/^{234}U), which was reasonable for the natural uranium sample. For more precise measurement, it is desirable to eliminate background noise which might contribute to the signal abundances detected in the full scan mass spectra. Once a sample containing intentionally enriched ^{235}U species was infused, the corresponding isotope ratio was

rapidly detected (Figure 7b) and provided solid evidence to specify the activities of uranium enrichment. Extra experiments showed that for a sample containing a minimal amount of enriched ^{235}U species (0.8%), the signal abundances of m/z 444 for 10 measurements were about 1152 ± 28 cps, which was differentiated from the signal levels (1010 ± 20 cps) of natural samples. These data show that EESI-MS is a convenient tool for rapid, sensitive detection of the isotope ratio of uranyl species. As demonstrated before, EESI can be implemented for in situ analysis without performance loss.[67] It is evident that a miniature mass spectrometer[68,69] installed with a specially designed EESI source for in situ analysis can be a good solution to screen the uranium enrichment spots on site, showing prospects for applications in homeland security and public safety programs.

Analysis Speed. Traditionally, multiple-step sample pretreatment is required prior to actual sample analysis using mass spectrometry-based techniques. Particularly, for trace detection of radioactive elements, sample pretreatment including extraction, separation, and preconcentration is usually required when using many techniques including mass spectrometry. With minimal sample pretreatment, ambient mass spectrometry has been successfully applied for rapid detection of organic compounds present in complex matrixes. As demonstrated in this study, inorganic species such as uranyl acetate in natural water samples were directly analyzed without sample separation, extraction, or preconcentration. A single sample analysis was completed within 1.5 min using MS^4. Currently, the throughput of this method was mainly limited by the sample loading and in-depth multiple-stage CID experiments. However, it takes only a few seconds to produce an EESI-MS spectrum of uranyl species in water with complex matrixes, showing that EESI-MS is a useful tool for high-throughput screening of uranyl species in liquids.

(67) Li, M.; Hu, B.; Li, J.; Chen, R.; Zhang, X.; Chen, H. W. *Anal. Chem.* **2009**, *81*, 7724–7731.

(68) Mulligan, C. C.; Justes, D. R.; Noll, R. J.; Sanders, N. L.; Laughlin, B. C.; Cooks, R. G. *Analyst* **2006**, *131*, 556–567.

(69) Gao, L.; Sugiarto, A.; Harper, J. D.; Cooks, R. G.; Ouyang, Z. *Anal. Chem.* **2008**, *80*, 7198–7205.

CONCLUSIONS

Extractive electrospray ionization mass spectrometry was successfully applied to characterize organic compounds in different complex matrixes without any sample pretreatment. In this work, an example of EESI-MS for rapid detection of radioactive inorganic species in natural water samples has been demonstrated. Under the experimental conditions, negatively charged uranyl acetate (m/z 447) undergoes characteristic fragmentation in the gas phase to produce UO_3^- as the final product, providing the fundamental chemistry for specific detection of uranyl acetate species in complex matrixes by EESI without sample pretreatment. Each single sample analysis was completed within 1.5 min using multiple stage CID experiments. The limit of detection was about a few 10^{-3} ng/L of uranium by utilizing the characteristic fragments obtained in the $EESI\text{-}MS^4$ experiments. This method provides reasonable relative standard deviation (RSD = 6.9∼8.1%) for 8 measurements (S/N = 3) and a linear dynamic range of 5 orders of magnitude. The isotope ratio of uranyl species can be rapidly detected, providing an alternative way to screen the spots used for uranium isotope separation and enrichment. Besides the fundamental importance, the results shown here establish a convenient method for fast detection of trace amounts of uranyl speciation, providing applications in analytical chemistry and technology development of uranium.

ACKNOWLEDGMENT

This work was jointly supported by the Innovation Method Fund of China (Grant No. 2008IM040400) and a grant from MOST of China (Grant 2009DFA41880).

Received for review August 28, 2009. Accepted November 6, 2009.

AC9019494